

# Temperature Dependence of $\text{Ca}^{2+}$ Wave Properties in Cardiomyocytes: Implications for the Mechanism of Autocatalytic $\text{Ca}^{2+}$ Release in Wave Propagation

Jutta Engel, Andrew J. Sowerby, Simon A. E. Finch, Martin Fechner, and Anton Stier

Max Planck Institute for Biophysical Chemistry, Department of Spectroscopy, 37018 Göttingen, Germany

**ABSTRACT** Digital imaging microscopy of fluo-3 fluorescence was used to study the velocity and shape of intracellular  $\text{Ca}^{2+}$  waves in isolated rat cardiomyocytes as a function of temperature. Decreasing the temperature from 37 to 17°C reduced the longitudinal wave velocity by a factor of 1.8 and remarkably slowed the decay of  $[\text{Ca}^{2+}]_i$  in the trailing flank of a wave. Using image analysis, rise times, and half-maximum decay times of local  $\text{Ca}^{2+}$  transients, which characterize the processes of local  $\text{Ca}^{2+}$  release and removal, were determined as a function of temperature. Apparent activation energies for wave front propagation, local  $\text{Ca}^{2+}$  release, and local  $\text{Ca}^{2+}$  removal were derived from Arrhenius plots and amounted to  $-23$ ,  $-28$ , and  $-46$  kJ/mol, respectively. The high activation energy of  $\text{Ca}^{2+}$  removal, which arises from the activity of the sarcoplasmic reticulum (SR)  $\text{Ca}^{2+}$  ATPase, relative to those of longitudinal wave propagation and local  $\text{Ca}^{2+}$  release excludes the hypothetical mechanism of regenerative “spontaneous  $\text{Ca}^{2+}$  release,” in which  $\text{Ca}^{2+}$  that has been taken up from the approaching wavefront triggers  $\text{Ca}^{2+}$  release at a luminal site of the SR. It is consistent, however, with the hypothesis that  $\text{Ca}^{2+}$  wave propagation is based on  $\text{Ca}^{2+}$ -induced  $\text{Ca}^{2+}$  release where  $\text{Ca}^{2+}$  triggers release on the cytosolic face of the SR.

## INTRODUCTION

During the last few years, considerable progress has been made in the understanding of spatio-temporal aspects of  $\text{Ca}^{2+}$  signaling because of the development of fluorescent  $\text{Ca}^{2+}$  dyes and the improvement of fluorescence imaging techniques. Propagating sites of elevated free  $\text{Ca}^{2+}$  concentration ( $[\text{Ca}^{2+}]_i$ ), so called  $\text{Ca}^{2+}$  waves, have been found in many different cell types (for review see Jaffe, 1993), among which are cardiomyocytes. Although it has remained unclear whether  $\text{Ca}^{2+}$  waves occur in normal cardiomyocytes in vivo (Lakatta, 1992) they have been intensively investigated (Takamatsu and Wier, 1990; Ishide et al., 1990, 1992; Wier and Blatter, 1991; Grouselle et al., 1991; Williams et al., 1992; Williams, 1993; Lipp and Niggli, 1993; Engel et al., 1994) because they yield information about the  $\text{Ca}^{2+}$  homeostasis of these cells. Another reason for studying  $\text{Ca}^{2+}$  waves is their possible involvement in pathological phenomena such as ischemia or arrhythmia (Stern et al., 1988; Lakatta, 1992; Fabiato, 1992).

$\text{Ca}^{2+}$  waves are generally assumed to propagate by regenerative coupling of autocatalytic release of  $\text{Ca}^{2+}$  from intracellular stores and  $\text{Ca}^{2+}$  diffusion (for review see Jaffe, 1993). The exact mechanism, however, by which  $\text{Ca}^{2+}$  waves propagate through cardiomyocytes has not been resolved. Two models of wave propagation (Wier and Blatter, 1991)

based on two types of autocatalytic  $\text{Ca}^{2+}$  release from the sarcoplasmic reticulum (SR), which were first observed in skinned cardiac cells and termed  $\text{Ca}^{2+}$ -induced  $\text{Ca}^{2+}$  release (CICR) and spontaneous  $\text{Ca}^{2+}$  release (SCR) (Fabiato, 1985a, b), exist.

CICR was defined as “ $\text{Ca}^{2+}$  release triggered by a rapid increase of  $[\text{Ca}^{2+}]_i$  to about  $0.6 \mu\text{M}$  at the outer surface of the SR of a previously quiescent skinned cell” (Fabiato, 1985a, b; 1992). The amount of  $\text{Ca}^{2+}$  released by CICR was found to be proportional to the rate of change of  $[\text{Ca}^{2+}]_i$  and to be inhibited at  $\text{Ca}^{2+}$  concentrations above  $1 \mu\text{M}$  (Fabiato, 1985a).

The second type of autocatalytic release of  $\text{Ca}^{2+}$  from the SR was observed when a skinned cell was exposed to a solution containing  $7 \mu\text{M}$   $\text{Ca}^{2+}$  (Fabiato, 1985b). In contrast to CICR, SCR occurred after a delay of up to several hundred milliseconds after increasing the  $\text{Ca}^{2+}$  concentration of the bath solution. SCR was thus explained to result from an overloaded SR in which  $\text{Ca}^{2+}$  triggered release at a luminal site of the SR. The delay in release was attributed to pumping  $\text{Ca}^{2+}$  inside the lumen by the SR  $\text{Ca}^{2+}$  ATPase (Fabiato, 1985a, b, 1992).

From these observations, it was concluded that “SCR and CICR do not occur through the same mechanism” (Fabiato, 1985b, 1992). The fact that the frequency of  $\text{Ca}^{2+}$  waves rises with increasing  $[\text{Ca}^{2+}]_i$  (Fabiato, 1985b, 1992; Stern et al., 1988; Grouselle et al., 1991; Williams et al., 1992) led to the interpretation that  $\text{Ca}^{2+}$  waves are merely a consequence of SR overload, i.e., based on SCR/diffusion coupling (Fabiato, 1985b, 1992). The mechanism of a wave relayed by SCR would be the following (Wier and Blatter, 1991):

- 1) Locally, overloaded SR spontaneously releases  $\text{Ca}^{2+}$ ;
- 2)  $\text{Ca}^{2+}$  released diffuses radially and is taken up by  $\text{Ca}^{2+}$  pumps into SR that is almost overloaded;

Received for publication 25 May 1994 and in final form 16 September 1994.

Address reprint requests to Dr. Jutta Engel, Georg August University, Institute of Physiology, Department of Neurophysiology, Humboldtallee 23, 37073 Göttingen, Germany. Tel.: 49-551-395913; Fax: 49-551-395923; E-mail: je@helena.ukps.gwdg.de.

Dr. Engel's current address: Georg August University, Institute of Physiology, Dept. of Neurophysiology, Humboldtallee 23, 37073 Göttingen, Germany.

© 1995 by the Biophysical Society

0006-3495/95/01/40/06 \$2.00

- 3) In these parts of the SR, SCR is triggered, and steps 1–3 repeat;
- 4)  $\text{Ca}^{2+}$  is pumped back into the SR.

The alternative model for  $\text{Ca}^{2+}$  wave propagation is based on the coupling of CICR and diffusion as follows:

- 1) Locally,  $[\text{Ca}^{2+}]_i$  rises because of influx through the sarcolemma, or an overloaded part of the SR spontaneously releases  $\text{Ca}^{2+}$ ;
- 2) This  $\text{Ca}^{2+}$  reaches SR release channels by diffusion, triggers  $\text{Ca}^{2+}$  release by acting at the outside of the SR, and the whole process repeats;
- 3)  $\text{Ca}^{2+}$  is pumped back into SR by  $\text{Ca}^{2+}$  ATPases.

The SCR hypothesis has been a matter of controversy (Wier and Blatter, 1991; Stern, 1992; Jaffe, 1993; Williams, 1993). Unfortunately, it cannot be proven directly, because no technique of imaging the  $\text{Ca}^{2+}$  concentration inside the SR in situ with high temporal resolution is available so far. Recently, we have studied the anisotropy of  $\text{Ca}^{2+}$  wave propagation in cardiomyocytes (Engel et al., 1994). By investigating the temperature dependence of transverse and longitudinal wave velocity, we tried to find out whether different direction-dependent processes cause anisotropic wave propagation. Here we characterize several wave parameters in more detail to compare their temperature dependence and to gain support for one of the above delineated models of wave propagation. It turns out that the velocity of wave propagation is much less affected by a decrease in temperature than is the rate of  $\text{Ca}^{2+}$  reuptake into the SR, suggesting that  $\text{Ca}^{2+}$  triggers autocatalytic  $\text{Ca}^{2+}$  release on a cytosolic rather than luminal site of the SR.

## MATERIALS AND METHODS

### Preparation of cells and labeling

Ventricular cardiomyocytes were isolated from adult Sprague-Dawley rats by Langendorff perfusion with collagenase solution as described previously (Engel et al., 1994). Cells were plated into plastic dishes where they attached to glass coverslips; they were used within 30 h. The cells were loaded with 2  $\mu\text{M}$  Fluo-3 AM (Molecular Probes, Eugene, OR) for 30 min at 22°C, washed, and incubated for 1 h to allow for dye hydrolysis. Coverslips were mounted into a 20  $\mu\text{l}$  perfusion chamber and continuously superfused with a HEPES buffer (in mM): NaCl 125, KCl 2.6,  $\text{CaCl}_2$  1,  $\text{MgSO}_4$  1.2, glucose 10, HEPES 20, pH 7.4, 300 mOsm. For measurements at 17°C, the room was cooled by air conditioning. Otherwise, chamber and microscope stage were heated to 27 or 37°C with an air stream incubator (Zeiss, Oberkochen, Germany).

### $\text{Ca}^{2+}$ measurements

On binding  $\text{Ca}^{2+}$ , the fluorescence intensity of fluo-3 changes by a factor of 40 (Minta et al., 1989). Therefore, an increase in fluorescence intensity corresponds to an increase in  $[\text{Ca}^{2+}]_i$ . Measurements of fluo-3 fluorescence were performed as described previously (Engel et al., 1994). Briefly, a Zeiss Axiomat was used in the epifluorescence mode with the 488 nm line of an argon laser (Series 2000, Spectra Physics, Mountain View, CA) as light source. Emitted fluorescence was detected by a low light level intensifying video camera (VIM C2400, Hamamatsu Photonics Europa GmbH, Seefeld, Germany). Images were acquired at video rate (25 Hz interlaced) and recorded on video tape by a SuperVHS video recorder (Panasonic; Matsushita

Electric Industrial Co., Osaka, Japan). Video frames were digitized by a frame grabber (VTE Digital Braunschweig, Germany) and transferred to a Silicon Graphics Workstation 4D/35 (Silicon Graphics Inc., Mountain View, CA). Processing of the images (512x795 pixels, 8 bit) was carried out with user-written routines based on the software IDL (Research Systems Inc., Boulder, CO). Each series of images displaying a  $\text{Ca}^{2+}$  wave (varying from 25 to 65 images) was scaled between pixel intensity 0 (background fluorescence) and 255 (maximum fluorescence in that series). Shaded surface plots and fluorescence intensity profiles were obtained after smoothing the images using a box car averaging procedure of 8 or 11 pixels (1.4 or 1.9  $\mu\text{m}$ ) width, respectively.

## RESULTS

Fluo-3-loaded myocytes were monitored for spontaneously generated  $\text{Ca}^{2+}$  waves at 17, 27 or 37°C for 2 min. Each cell was subjected to only one temperature to exclude possible side effects of fast temperature changes on its  $\text{Ca}^{2+}$  homeostasis. At each temperature, cells of at least three different preparations were examined. Only cells with clear morphology (without branches) that exhibited linear, longitudinal  $\text{Ca}^{2+}$  waves were selected for evaluation.

$\text{Ca}^{2+}$  waves were observed at all temperatures examined. Changing the temperature from 37 to 17°C affected both wave velocity and shape. Fig. 1 shows longitudinal  $\text{Ca}^{2+}$  waves in isolated myocytes recorded at 37°C and at 17°C as surface plots i.e. the fluorescence intensity of fluo-3 is encoded in the height of the surface. Both  $\text{Ca}^{2+}$  waves started at one end of the cell and traveled to the opposite end where they disappeared. The wave recorded at 37°C traveled much faster than that recorded at 17°C (93  $\mu\text{m/s}$  versus 46  $\mu\text{m/s}$ ). In addition, the waves differed markedly in their length: the wave at 17°C was much longer than that at 37°C, indicating that the removal of  $\text{Ca}^{2+}$  from the cytosol was considerably slower at 17°C.

In order to compare wave shapes as a function of temperature, longitudinal sections through fluorescence images of cells exhibiting linear  $\text{Ca}^{2+}$  waves from one end to the other were made. Fig. 2 shows wave propagation in terms of series of longitudinal fluorescence intensity profiles in three cells at 17, 27, and 37°C. The temporal distance between consecutive fluorescence profiles varies from 120 ms for the wave recorded at 37°C (A) to 240 ms for the one recorded at 17°C (C) because of the temperature-dependent slowing of wave propagation. Wave velocities are 99, 86, and 63  $\mu\text{m/s}$  at 37, 27, and 17°C, respectively.

Changing the temperature from 37 to 17°C decreased the slope of the  $[\text{Ca}^{2+}]_i$  increase at the wave front only slightly. However, the extension of the wave crest increased remarkably. Having left the focus, all three waves traveled at relatively constant width—30, 46, and 72  $\mu\text{m}$  at 37, 27, and 17°C, respectively—through the cell. This indicates that  $\text{Ca}^{2+}$  removal on the trailing edge of the wave is very sensitive to changes in temperature.

To quantify the processes of  $\text{Ca}^{2+}$  release and removal in  $\text{Ca}^{2+}$  waves, we analyzed the kinetics of local  $\text{Ca}^{2+}$  transients (Fig. 3). For this purpose, cross sections through fluorescence images of cardiomyocytes were defined and the fluorescence intensity was integrated along this line (width 1

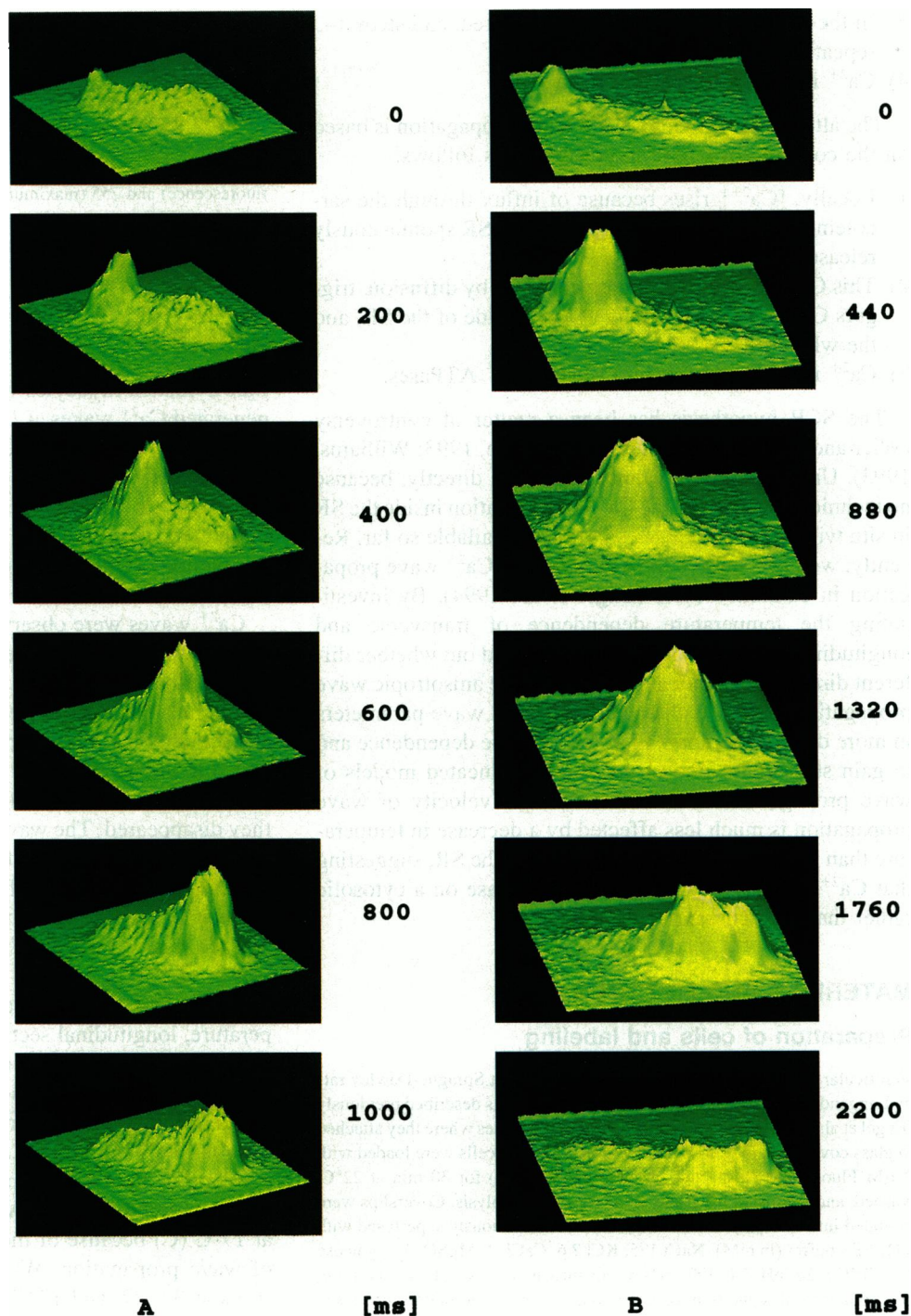


FIGURE 1 Propagation of  $\text{Ca}^{2+}$  waves in fluo-3-loaded cardiomyocytes under normothermic ( $37^\circ\text{C}$ , A) and hypothermic ( $17^\circ\text{C}$ , B) conditions. Consecutive surface plots of fluorescence intensity of scaled images are shown. Times (in ms) are respectively indicated in the right margin. Side lengths of the image planes are 140 and  $94\ \mu\text{m}$ .

pixel, Fig. 3 A, *inset*) as a function of time. This yielded the local kinetics of  $\text{Ca}^{2+}$  release and removal. Fig. 3 A shows local transients of three typical  $\text{Ca}^{2+}$  waves at 37, 27, and  $17^\circ\text{C}$ . The rate of  $\text{Ca}^{2+}$  release was less affected by a temperature change than that of  $\text{Ca}^{2+}$  removal. To describe the process of  $\text{Ca}^{2+}$  release, we used the local rise time,  $t_r$ , which is the time span from the beginning of fluorescence increase to maximum fluorescence as shown in the sketch in Fig. 3 B. To characterize the process of  $\text{Ca}^{2+}$  removal, the half-maximum decay time of fluorescence intensity,  $t_{1/2}$ , was chosen (Fig. 3 B).

A summary of the dependences of characteristic  $\text{Ca}^{2+}$  wave parameters such as longitudinal wave velocity,  $v_l$ , local rise time,  $t_r$ , and local half-maximum decay times,  $t_{1/2}$ , upon temperature is given in Table 1. Wave velocities were obtained as described previously (Engel et al., 1994). Rise time and half-maximum decay time were determined in triplicate from each cell by using fluorescence integrals from three equidistant transverse sections (which divided a cell in 4 parts) and were averaged. From Table 1 follows that propagation velocity decreased by a factor of 1.8 upon decreasing the temperature from 37 to

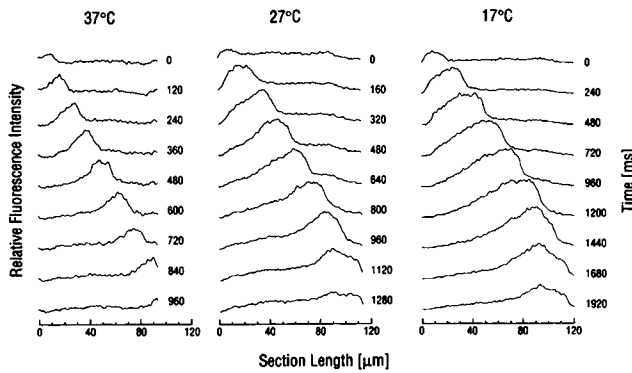


FIGURE 2 Longitudinal propagation of three representative Ca<sup>2+</sup> waves recorded at 37, 27, and 17°C (A–C). Fluorescence intensity profiles obtained along a central longitudinal section in every cell are plotted for different times. Note that the temporal distance between consecutive intensity profiles is different for the three temperatures because of considerable slowing of both wave velocity and wave decay on lowering the temperature.

17°C, whereas the local decay time was much more affected, being 3.5-fold increased.

To compare the dependences of wave propagation velocity, Ca<sup>2+</sup> release, and Ca<sup>2+</sup> removal upon temperature, Arrhenius plots were derived from the data given in Table 1. In general, an Arrhenius plot shows the dependence of a reaction time constant on a logarithmic scale upon the inverse temperature. Unfortunately, the processes mentioned above are rather complex and cannot be described by single reaction time constants. Nevertheless, an Arrhenius plot of a catenated series of reactions can often yield useful information about rate-limiting reaction steps (Johnson et al., 1974). Here we used the longitudinal wave velocity, the rise time constant,  $k_r = 1/t_r$ , and the half-maximum decay time constant,  $k_{1/2} = 1/t_{1/2}$ , to describe the complex processes of wave propagation, local Ca<sup>2+</sup> release, and local Ca<sup>2+</sup> removal. Fig. 4 shows that the logarithms of the mean values of  $v_l$ ,  $k_r$ , and  $k_{1/2}$  could be approximated by straight lines in the temperature range 17–37°C. Apparent activation energies  $E_a$  were calculated from the slope of the regression line according to the Arrhenius equation:

$$k = k_0 \exp(-\Delta E_a/RT), \quad (1)$$

with  $k$  being the time constant of the respective process,  $k_0$  a constant,  $R$  the gas constant, and  $T$  the absolute temperature (Johnson et al., 1974). Apparent activation energies were  $-23$  kJ/mol for longitudinal wave propagation,  $-28$  kJ/mol for local Ca<sup>2+</sup> release, and  $-46$  kJ/mol for local Ca<sup>2+</sup> removal.

## DISCUSSION

In this study we have analyzed the temperature dependence of three parameters of a Ca<sup>2+</sup> wave: longitudinal wave velocity, rise time constant, and half-maximum decay time constant of the local Ca<sup>2+</sup> transient. Our aim was to compare the temperature dependences of wave front propagation velocity

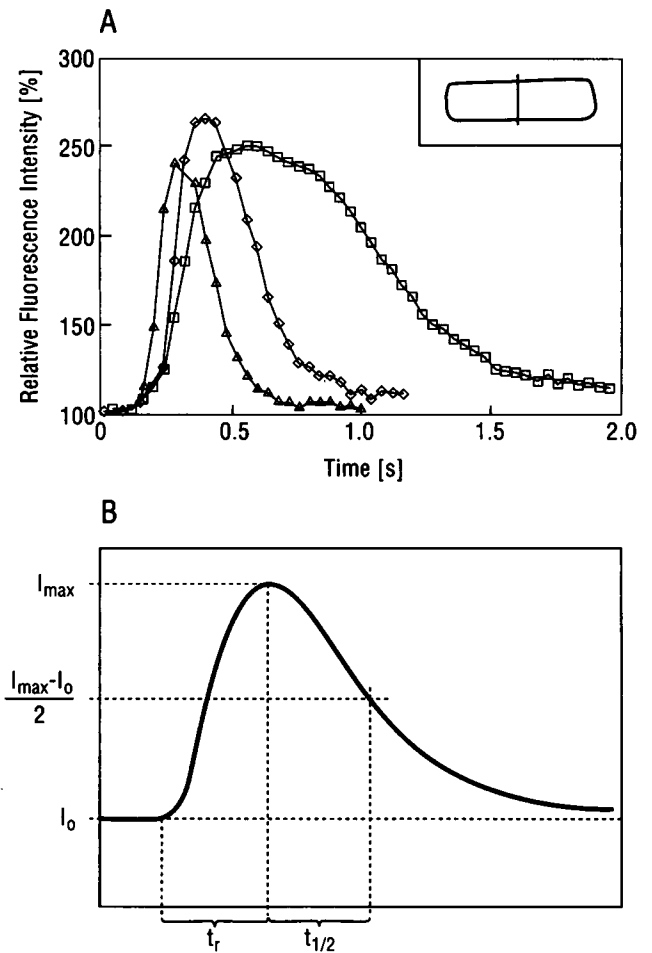


FIGURE 3 Temperature dependence of local Ca<sup>2+</sup> release and reuptake kinetics in Ca<sup>2+</sup> waves. (A) In three representative cells, the fluorescence intensity was integrated along a central cross section of the cell (see insert) as a function of time. Symbols refer to different temperatures: ( $\Delta$ ) 37, ( $\diamond$ ) 27, and ( $\square$ ) 17°C. (B) Schematic representation of a local Ca<sup>2+</sup> transient in A to illustrate the definition of local rise time,  $t_r$ , and half-maximum decay time,  $t_{1/2}$ .

TABLE 1 Temperature dependence of mean longitudinal wave velocity, mean rise time, and mean half-maximum decay time of the local Ca<sup>2+</sup> transient

Temperature (°C)	Longitudinal velocity ( $v_l$ ) ( $\mu\text{m/s}$ )	Rise time ( $t_r$ ) (ms)	Half-maximum decay time ( $t_{1/2}$ ) (ms)
17	56 $\pm$ 16 (18)	356 $\pm$ 31 (13)	597 $\pm$ 169 (13)
27	75 $\pm$ 11 (20)	259 $\pm$ 45 (14)	288 $\pm$ 79 (14)
37	103 $\pm$ 14 (17)	169 $\pm$ 24 (15)	172 $\pm$ 34 (15)

For definition of  $t_r$  and  $t_{1/2}$ , see Fig. 3 B. Data represent mean  $\pm$  SD (number of waves).

and of the process of local Ca<sup>2+</sup> release with the process of active Ca<sup>2+</sup> reuptake by the SR, and to decide whether Ca<sup>2+</sup> waves propagate by a mechanism in which Ca<sup>2+</sup> regeneratively triggers Ca<sup>2+</sup> release from an overloaded SR at a luminal site.

Each of the three wave parameters arises from several elementary processes rather than describing a single

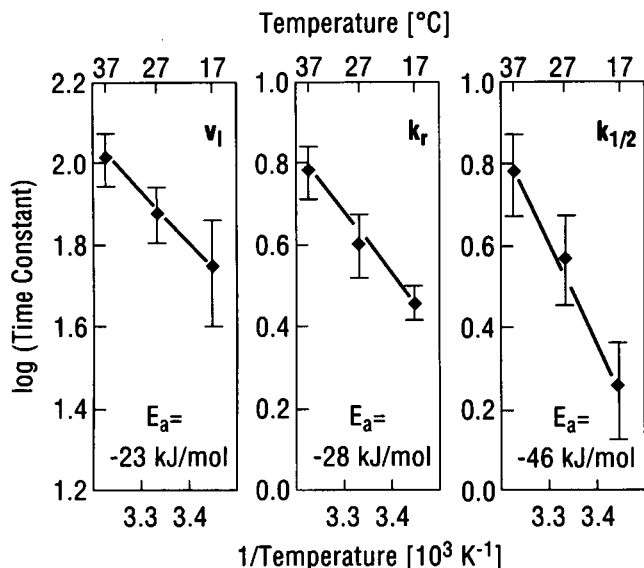


FIGURE 4 Arrhenius plots of longitudinal wave velocity  $v_l$  (left), rise time constant  $k_r$  (center), and decay time constant  $k_{1/2}$  (right). Linear regression yielded the apparent activation energies indicated in the plots.

chemical reaction: the rise time constant,  $k_r$ , mainly reflects local  $\text{Ca}^{2+}$  release from the SR caused by previous binding of  $\text{Ca}^{2+}$  to a catalytic (cytosolic or luminal) site of the ryanodine receptor. Its apparent activation energy of  $-28$  kJ/mol arises from the combination of at least two processes: channel opening and ion flow. Activation energies of channel opening, which involve conformational changes, may be quite high ( $-80$  kJ/mol, Hille, 1992). In contrast, ion flow through an ion channel has a comparatively low activation energy of about  $-20$  to  $-30$  kJ/mol (Hille, 1992). This suggests that the flow of  $\text{Ca}^{2+}$  ions through the channel is the rate-limiting step in the temperature range considered.

The second local parameter,  $k_{1/2}$ , summarizes  $\text{Ca}^{2+}$  reuptake into the SR by the SR  $\text{Ca}^{2+}$  ATPase and  $\text{Ca}^{2+}$  extrusion out of the cell. The latter process occurs mainly via the  $\text{Na}^+/\text{Ca}^{2+}$  exchanger (Sipido and Wier, 1991). Unfortunately, the ratio of the transport capacities of the two processes in a  $\text{Ca}^{2+}$  wave is not known. From experiments with electrically stimulated cardiomyocytes, it has been estimated that less than 25% of the total  $\text{Ca}^{2+}$  in a  $\text{Ca}^{2+}$  transient enters the cell during depolarization, whereas 75–90% is released from the SR (Bers and Bridge, 1989; Sipido and Wier, 1991). Hence, in the steady state about 20% of the  $\text{Ca}^{2+}$  must be extruded from the cell after each stimulation (Powell and Noble, 1989). This percentage is probably even less in a  $\text{Ca}^{2+}$  wave. For simplicity, we will neglect  $\text{Ca}^{2+}$  extrusion from the cell in the following discussion, so  $k_{1/2}$  is assumed to reflect only the activity of the  $\text{Ca}^{2+}$  ATPase of the SR. This is supported by the notion that its activation energy is in the same range as that determined for pumping  $\text{Ca}^{2+}$  by the SR  $\text{Ca}^{2+}$  ATPase ( $-49$  kJ/mol, Squier et al., 1988), suggesting that  $k_{1/2}$  reflects the activity of this enzyme.

Finally, the longitudinal velocity of a  $\text{Ca}^{2+}$  wave depends on the rate of  $\text{Ca}^{2+}$  release and the amount of  $\text{Ca}^{2+}$  released at each site, on the distance between successive release re-

gions, and on the effective diffusion coefficient for  $\text{Ca}^{2+}$  in the myoplasm (Stern, 1992). Unfortunately, quantitative data regarding the regulation of the release channels and their ultrastructural organization are still rather limited. For simplicity, we consider a  $\text{Ca}^{2+}$  wave in a myocyte as a chemical wave in an excitable medium. The longitudinal velocity of such a wave is given approximately by

$$v_l \sim (k_{as}D)^{1/2}, \quad (2)$$

where  $k_{as}$  is the rate constant of the autocatalytic step and  $D$  is the diffusion coefficient of the autocatalytic species (Tilden, 1974; Kuhnert et al., 1985; Foerster et al., 1990). Taking into account the temperature dependence of  $D$  and  $k_{as}$ , respectively, one arrives at

$$E_v = \frac{1}{2}(E_d + E_{as}), \quad (3)$$

where  $E_v$  is the apparent activation energy of longitudinal wave propagation,  $E_d$  the activation energy of diffusion, and  $E_{as}$  the activation energy of the autocatalytic step (Kuhnert et al., 1985; Foerster et al., 1990). It is interesting to note that when inserting  $E_v = -23$  kJ/mol from the Arrhenius plot (Fig. 4 A) and  $E_d = -18$  kJ/mol for  $\text{Ca}^{2+}$  diffusion (Erdey-Grüz, 1974) in Eq. 3, one arrives at  $E_{as} = -28$  kJ/mol, a value we found experimentally for the apparent activation energy of local  $\text{Ca}^{2+}$  release (Fig. 4 B). This suggests that despite the complex ultrastructure of the cytoplasm, it may be useful to apply the theory of chemical waves to cytoplasmic second messenger waves, as has been done successfully for  $\text{Ca}^{2+}$  waves in oocytes (Lechleiter and Clapham, 1992).

In the SCR model, autocatalytic  $\text{Ca}^{2+}$  release is triggered at a luminal site of the SR. This requires that at the front of the  $\text{Ca}^{2+}$  wave,  $\text{Ca}^{2+}$  has first to be taken up by the SR, where it triggers release above a certain threshold concentration of luminal  $\text{Ca}^{2+}$ . According to this model and in view of the high activation energy of  $\text{Ca}^{2+}$  pumping into the SR, one expects that both local  $\text{Ca}^{2+}$  release and wave velocity are similarly affected by a decrease in temperature as is the rate of  $\text{Ca}^{2+}$  reuptake. However, this is not the case: propagation velocity decreases by a factor of only 1.8 and the rate of local  $\text{Ca}^{2+}$  release by a factor of 2.1, whereas the reuptake rate decreases by a factor of 3.5 on changing the temperature from 37 to 17°C. We thus conclude that SCR is not the mechanism of regenerative  $\text{Ca}^{2+}$  wave propagation. In contrast, the results presented here support the CICR hypothesis, i.e., that  $\text{Ca}^{2+}$  release is triggered at a cytosolic site of the SR release channel.

The experiments with skinned cardiac cells (Fabiato, 1985b, 1992) mentioned in the Introduction, as well as the fact that the frequency of  $\text{Ca}^{2+}$  waves rises with an increasing cytosolic  $\text{Ca}^{2+}$  concentration—which certainly also leads to a higher luminal  $\text{Ca}^{2+}$  concentration (Grouselle et al., 1991; Williams et al., 1992)—suggest that SCR does exist in cardiomyocytes. It seems likely that SCR initiates  $\text{Ca}^{2+}$  waves by spontaneous local  $\text{Ca}^{2+}$  release from an overloaded part of the SR, whereas propagation of the wave is based on regenerative CICR. Interestingly, CICR does not seem to be

independent of the luminal  $\text{Ca}^{2+}$  concentration. A certain supranormal  $\text{Ca}^{2+}$  SR load has been reported to be necessary to support wave propagation (Trafford et al., 1993). Theoretical considerations (Stern, 1992) indicate that the loading state of the SR might also modulate CICR in that differences in the loading state of the SR may be responsible for the variety of  $\text{Ca}^{2+}$  amplitudes and propagation velocities seen in  $\text{Ca}^{2+}$  waves at a given temperature.

We wish to thank Bianca Kellner and Caterina Habermann for excellent technical assistance and Stefan C. Müller, Thomas Heimbürg, and Detlev Schild for stimulating discussions.

This work was supported by the Deutsche Forschungsgemeinschaft (SFB 330) and the Association for International Cancer Research (U.K.).

## REFERENCES

- Bers, D. M., and J. H. Bridge. 1989. Relaxation of rabbit ventricular muscle by Na-Ca exchange and sarcoplasmic reticulum calcium pump. *Circ. Res.* 65:334–342.
- Engel, J., M. Fechner, A. J. S. Sowerby, S. A. E. Finch, and A. Stier. 1994. Anisotropic propagation of  $\text{Ca}^{2+}$  waves in isolated cardiomyocytes. *Biophys. J.* 66:1756–1762.
- Erdey-Grüz, T. 1974. Transport Phenomena in Aqueous Solutions. Adam Hilger, London. 194 pp.
- Fabiato, A. 1985a. Time- and calcium dependence of activation and inactivation of calcium-induced release of calcium from the sarcoplasmic reticulum of a skinned canine cardiac Purkinje cell. *J. Gen. Physiol.* 85:247–289.
- Fabiato, A. 1985b. Simulated calcium current can both cause calcium loading in and trigger calcium release from the sarcoplasmic reticulum of a skinned canine cardiac Purkinje cell. *J. Gen. Physiol.* 85:291–320.
- Fabiato, A. 1992. Two kinds of calcium-induced release of calcium from the sarcoplasmic reticulum of skinned cardiac cells. In *Excitation-Contraction Coupling in Skeletal, Cardiac and Smooth Muscle*. G. B. Frank, editor. Plenum Press, New York. 245–262.
- Foerster, P., S. C. Müller, and B. Hess. 1990. Temperature dependence of curvature-velocity relationship in an excitable Belousov-Zhabotinskii reaction. *J. Phys. Chem.* 94:8859–8861.
- Grouselle, M., B. Stuyvers, S. Bonoron-Adele, P. Besse, and D. Georgescauld. 1991. Digital-imaging microscopy analysis of calcium release from sarcoplasmic reticulum in single rat cardiac myocytes. *Pflügers Arch.* 418:109–119.
- Hille, B. 1992. *Ionic Channels of Excitable Membranes*. Sinauer Associates Inc., Sunderland, MA. 50 pp., 329 pp.
- Ishide, N., M. Miura, M. Sakurai, and T. Takishima. 1992. Initiation and development of calcium waves in rat myocytes. *Am. J. Physiol.* 263: H327–H332.
- Ishide, N., T. Urayama, K. I. Inoue, T. Komaru, and T. Takishima. 1990. Propagation and collision characteristics of calcium waves in rat myocytes. *Am. J. Physiol.* 259:H940–H950.
- Jaffe, L. F. 1993. Classes and mechanisms of calcium waves. *Cell Calcium* 14:736–745.
- Johnson, F. H., H. Eyring, and B. J. Stover. 1974. *The Theory of Rate Processes in Biology and Medicine*. John Wiley & Sons, New York. 169 pp.
- Kuhnert, L., H.-J. Krug, and L. Pohlmann. 1985. Velocity of trigger waves and temperature dependence of autowave processes in the Belousov-Zhabotinsky reaction. *J. Phys. Chem.* 89:2022–2026.
- Lakatta, E. 1992. Functional implications of spontaneous sarcoplasmic reticulum  $\text{Ca}^{2+}$  release in the heart. *Cardiovasc. Res.* 26:193–214.
- Lechleiter, J. D., and D. Clapham. 1992. Molecular mechanisms of intracellular calcium excitability in *X. laevis* oocytes. *Cell.* 69:283–294.
- Lipp, P., and E. Niggli. 1993. Microscopic spiral waves reveal positive feedback in subcellular calcium signaling. *Biophys. J.* 65: 2272–2276.
- Minta, A., J. P. Y. Kao, and R. Y. Tsien. 1989. Fluorescent indicators for cytosolic calcium based on rhodamine and fluorescein chromophores. *J. Biol. Chem.* 264:8171–817.
- Powell, T., and D. Noble. 1989. Calcium movements during each heart beat. *Mol. Cell. Biochem.* 89:103–108.
- Sipido, K. R., and W. G. Wier. 1991. Flux of  $\text{Ca}^{2+}$  across the sarcoplasmic reticulum of guinea-pig cardiac cells during excitation-contraction coupling. *J. Physiol.* 435:605–630.
- Squier, T. C., D. J. Bigelow, and D. D. Thomas. 1988. Lipid fluidity directly modulates the overall protein rotational mobility of the Ca-ATPase in sarcoplasmic reticulum. *J. Biol. Chem.* 263:9178–9186.
- Stern, M. D. 1992. Theory of excitation-contraction coupling in cardiac muscle. *Biophys. J.* 63:497–517.
- Stern, M. D., M. C. Capogrossi, and E. G. Lakatta. 1988. Spontaneous calcium release from the sarcoplasmic reticulum in myocardial cells: mechanisms and consequences. *Cell Calcium.* 9:247–256.
- Takamatsu, T., and W. G. Wier. 1990. Calcium waves in mammalian heart: quantification of origin, magnitude, waveform, and velocity. *FASEB J.* 4:1519–1525.
- Tilden, J. 1974. On the velocity of spatial wave propagation in the Belousov reaction. *J. Chem. Phys.* 60:3349–3350.
- Trafford, A. W., S. C. O. O'Neill, and D. A. Eisner. 1993. Factors affecting the propagation of locally activated systolic Ca transients in rat ventricular myocytes. *Pflügers Arch.* 425:181–183.
- Wier, W. G., and L. A. Blatter. 1991.  $\text{Ca}^{2+}$ -oscillations and  $\text{Ca}^{2+}$ -waves in mammalian cardiac and vascular smooth muscle cells. *Cell Calcium.* 12:241–254.
- Williams, D. A. 1993. Mechanisms of calcium release and propagation in cardiac cells. Do studies with confocal microscopy add to our understanding? *Cell Calcium.* 14:724–735.
- Williams, D. A., L. M. Delbridge, S. H. Cody, P. J. Harris, and T. O. Morgan. 1992. Spontaneous and propagated calcium release in isolated cardiac myocytes viewed by confocal microscopy. *Am. J. Physiol.* 262: C731–C742.